ARTICLES

Atomic structures of amyloid cross-β spines reveal varied steric zippers

Michael R. Sawaya[1], Shilpa Sambashivan[1], Rebecca Nelson[1], Magdalena I. Ivanova[1], Stuart A. Sievers[1], Marcin I. Apostol[1], Michael J. Thompson[1], Melinda Balbirnie[1], Jed J. W. Wiltzius[1], Heather T. McFarlane[1], Anders Ø. Madsen[2,3], Christian Riekel[3] & David Eisenberg[1]

Amyloid fibrils formed from different proteins, each associated with a particular disease, contain a common cross-β spine. The atomic architecture of a spine, from the fibril-forming segment GNNQQNY of the yeast prion protein Sup35, was recently revealed by X-ray microcrystallography. It is a pair of β-sheets, with the facing side chains of the two sheets interdigitated in a dry 'steric zipper'. Here we report some 30 other segments from fibril-forming proteins that form amyloid-like fibrils, microcrystals, or usually both. These include segments from the Alzheimer's amyloid-β and tau proteins, the PrP prion protein, insulin, islet amyloid polypeptide (IAPP), lysozyme, myoglobin, α-synuclein and β_2-microglobulin, suggesting that common structural features are shared by amyloid diseases at the molecular level. Structures of 13 of these microcrystals all reveal steric zippers, but with variations that expand the range of atomic architectures for amyloid-like fibrils and offer an atomic-level hypothesis for the basis of prion strains.

Amyloid diseases are accompanied by the deposition of elongated, unbranched protein fibrils. For pathologists to designate a disease as amyloid, the fibrils must be deposited extracellularly, and must bind the dye Congo red, giving an 'apple-green' birefringence[1]. As of 2005, Alzheimer's disease and some 24 others have been found to satisfy this stringent definition[1,2]. In addition, many other proteins have been found to form amyloid-like fibrils with biophysical properties in common with amyloid fibrils. These properties include an elongated morphology[3], binding of Congo red, formation from their constituent protein molecules with cooperative, nucleation-dependent kinetics[4], and the so-called cross-β X-ray diffraction pattern[5–7]. This pattern consists of an X-ray reflection at ~4.8 Å resolution along the fibril direction, and another X-ray reflection at ~8–11 Å resolution perpendicular to the fibril direction[5,8,9]. The pattern reveals that the fibrils contain β-sheets parallel to the fibril axis, with their extended protein strands perpendicular to the axis.

Finding atomic-level structures for cross-β spines has been impeded by the fibrillar nature of amyloid, but the corner has been turned. Recent progress has included models for fibrillar segments constrained by chemical labelling, scanning proline mutagenesis, electron paramagnetic resonance, NMR, H/D exchange and X-ray fibre diffraction data[10–21], and two atomic-resolution microcrystal structures of the fibril-forming segments GNNQQNY and NNQQNY[22] from the yeast prion protein Sup35. Here we extend atomic-resolution crystallographic studies to other fibril-forming segments taken from disease-related proteins, and we relate the segments to the fibrils formed by their parent proteins.

Peptide microcrystals and fibrils

Our study of the overlapping segments GNNQQNY and NNQQNY[22–24] showed that short peptides can themselves form both fibrils and closely related microcrystals, the latter capable of revealing atomic structures. From these structures, it was evident how short segments form fibrils: the cross-β spine consists of a pair of β-sheets; each sheet is formed from extended strands of the segment, hydrogen-bonding up and down the sheet to identical molecules, all perpendicular to the axis of the fibril. Two sheets mate tightly at a completely dry interface. At this interface, the residue side chains intermesh with close complementarity, in what we term a steric zipper. The pair-of-sheets motif, with its dry, steric-zipper interface repeated along the entire length of the needle-shaped crystal, accounts for the elongated shape of the crystal and presumably of the fibril. In fibrils formed from full proteins, the extra-spine regions may remain on the periphery of the spine, in some cases in native-like conformation[25,26].

These initial results encouraged us to identify fibril-forming segments in other disease-related and fibril-forming proteins, and to determine structures for these new cross-β spines. In fact, in this class of proteins, we have identified one or more such segments in every protein we examined. Identification of these segments was based on a combination of bioinformatic and experimental procedures[23,27–29], guided in some cases by the published work of others. So far we have identified some 30 such segments from 14 different proteins (see Supplementary Table 1). Most of these fibril-forming segments also form needle-shaped microcrystals, varying in length but rarely larger than 2×2 μm in cross section (Fig. 1). Several control segments, predicted not to form fibrils, did not form fibrils[29]. The wide variety of protein sequences that form fibrils ranges from highly polar (for example, NNQQ) to highly apolar (for example, MVGGVV), and from small side chains (for example, SSTSAA) to large (for example, FYLLYY). Despite their variation, these sequences have a property in common: their self-complementary binding.

Fibrils related to microcrystals

Although the 13 segment structures are known with high accuracy (resolutions between 0.85 and 2.0 Å and *R*-factors between 0.07 and 0.24), there is lingering uncertainty as to how reflective these structures are of amyloid fibrils. Three types of evidence suggest that the crystal structures of segments we report here are related to structures of the fibrils formed by the same segment, and also to fibrils formed from the entire proteins from which the segments are taken.

[1]Howard Hughes Medical Institute, UCLA-DOE Institute of Genomics and Proteomics, Los Angeles, California 90095-1570, USA. [2]Centre for Crystallographic Studies, Department of Chemistry, University of Copenhagen, Universitetsparken 5, DK-2100 KBH, Denmark. [3]European Synchrotron Radiation Facility, BP 220, F-38043 Grenoble Cedex, France.

Structural similarities of microcrystals to fibrils. Microcrystals and fibrils often grow under the same conditions, and are sometimes found together in solution. Some fibrils (Fig. 1b, c) appear to grow from tips of microcrystals. In all of the segment crystals, the segment fibrils, and the fibrils of whole proteins that we have tested, β-strands are the principal diffracting feature. The strands extend perpendicular to the long axis of the crystal and of the fibrils. Also, the inter-sheet spacings and interstrand spacings of our crystals are in general accord with the spacings found in amyloid fibrils by X-ray fibre diffraction[7,30]. We show this systematically for microcrystals of segments from Sup35 and amyloid-β protein in Supplementary Fig. 1. This figure compares X-ray fibril diffraction patterns of the full proteins with simulated fibril patterns from our microcrystals, produced by cylindrical averaging of the single microcrystal X-ray data. The comparison shows a good fit of the principal diffraction features, suggesting that the principal structural features of the protein fibrils are closely similar to those within the microcrystals.

Nucleation experiments. Nucleated growth is one of the hallmarks of amyloid fibrils[31], and amyloid nucleation requires equivalence of the molecular structures of the nucleus and the fibril[32]. To study nucleated growth, we prepared crystalline seeds from the insulin segment LVEALYL, from which we have determined the steric-zipper structure of VEALYL. These seeds shorten the characteristic lag time for the growth of insulin fibrils as much as seeds prepared from fibrils of the entire insulin molecule (Supplementary Fig. 2), whereas a non-fibril-forming segment of insulin fails to shorten the lag time. This is strong evidence for the involvement of LVEALYL in insulin fibrils. We also found that full-length Sup35 accelerates GNNQQNY peptide aggregation[23]. Both studies suggest a structural similarity between peptide segments and fibrils of their parent proteins.

Mutations in fibril-forming segments affect fibril formation of whole proteins. If the segments of our structures are in fact in the amyloid spines of their parent proteins, we would expect that mutations in the segments would diminish fibril formation, and that these segments would show enhanced protection from proton exchange. In fact, as detailed in Supplementary Table 2, work of others has established that mutants within eight of these segments either slow or diminish fibril formation. Other studies have found that three of our segments lie in regions of fibrils that show protection to proton exchange.

In summary, diffraction patterns show that the principal diffracting features of protein fibrils and the corresponding microcrystals are closely similar; the ability of the protein segments to seed fibrils of their parent proteins shows that these segments are involved in protein fibril formation and probably have similar atomic arrangements in microcrystals and protein fibrils; and the fact that mutant sequences of the microcrystalline segments affect fibril formation of their parent proteins suggests that these segments are involved in protein fibril formation. Although none of these experiments proves that the structure of the microcrystal is the same as that of their corresponding protein fibrils, the evidence indicates a structural similarity.

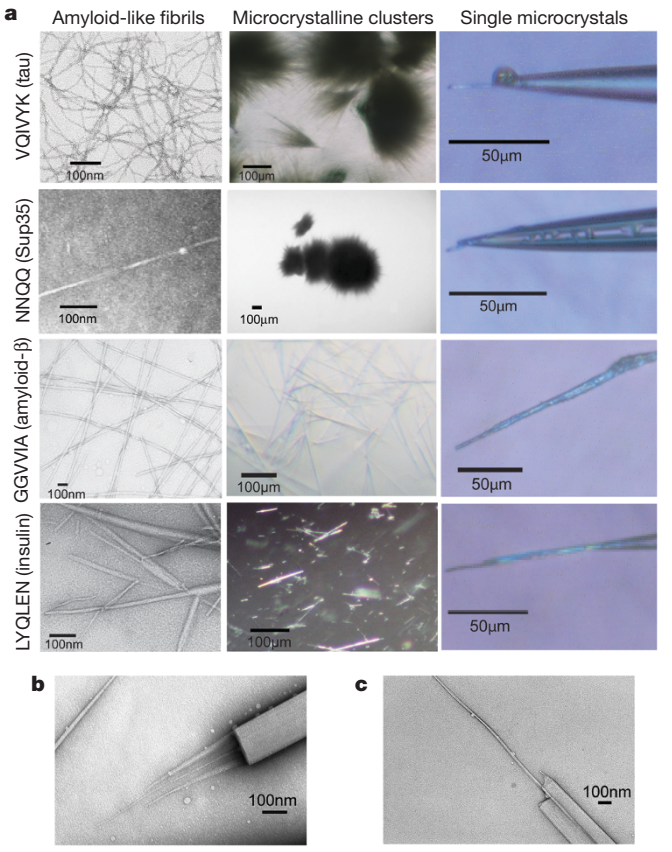

Figure 1 | Amyloid fibrils and microcrystals. a, Electron micrographs of representative amyloid-like fibrils (left), and magnified images of microcrystalline clusters (middle) and single microcrystals mounted for X-ray diffraction (right) of four segments identified from fibril-forming proteins: VQIVYK from tau, NNQQ from Sup35, GGVVIA from amyloid-β, and LYQLEN from insulin. **b**, **c**, Microcrystals of fibril-forming segments of amyloid-forming proteins, appearing to have fibrils growing from their tips. Shown are negatively stained transmission electron micrographs of a microcrystal of segment NFLVHSS from IAPP (**b**), and of VEALYL from insulin (**c**). In both panels, the microcrystals are on the right.

Eight classes of steric zippers

Although varied in sequence, all of our 11 new high-resolution microcrystal structures (Figs 2, 3; Supplementary Table 3; and Supplementary Fig. 3) resemble those of GNNQQNY and NNQQNY[22] in containing extended protein strands that are perpendicular to the needle axes and organized into standard Pauling–Corey β-sheets. Because every one of the structures is built around the steric zipper that we found previously in GNNQQNY and NNQQNY[22], the structures suggest that dry, steric-zipper interfaces between β-sheets are a general principle of protein complementation in amyloid structures. Other examples of extended protein or peptide chains forming such steric-zipper interfaces between protein chains are essentially absent from the PDB (Protein Data Bank) and are rare in the CSD (Cambridge Structural Database), supporting the idea that these interfaces are the defining molecular property of the amyloid state.

Despite their fundamental similarity, the reported structures display variations of the basic steric-zipper structure and thereby expand our understanding of amyloid structure. The structures to date fall into five classes (Figs 2, 3), distinguished by (1) whether their sheets (that is, the strands in their sheets) are parallel or antiparallel, (2) whether sheets pack with the same ('face-to-face') or different ('face-to-back') surfaces adjacent to one another, and (3) whether the sheets are oriented parallel ('up–up') or antiparallel ('up–down') with respect to one another. To distinguish this third type of orientation from the first, we refer to the relative sheet orientations in terms of a given sheet edge facing 'up' or 'down.' Combinations of these three structural arrangements give eight theoretically possible classes of steric zippers, shown in Fig. 4. Examples of classes 1, 2, 4, 7 and 8 are represented in our 13 microcrystal structures (Figs 2, 3).

The steric zippers of class 1 share a basic unit of two parallel, in-register β-sheets with their same sides facing each other ('face-to-face') and both sheet edges facing 'up'. Each sheet is related to its mate by a 2_1 axis parallel to the needle axis of the crystal, which rotates a sheet by 180° about the axis and moves it along the axis by half the spacing between two β-strands (Fig. 3, far left). This symmetry allows the side chains of one sheet to nestle between layers of side chains on the mating sheet, forming the steric zipper. In class 2, the symmetry is a simple translation of one sheet onto its neighbour, resulting in a

'face-to-back, up–up' packing. SNQNNF, from the human prion protein, is thus far the only example of a class 2 zipper. In class 4, like class 2, the apposed, interdigitating faces of the sheets differ from each other ('face-to-back'). However, neighbouring sheets of class 4 are oriented with one sheet's edge facing 'up' and its neighbours' edges 'down'. GGVVIA, from the carboxy terminus of amyloid-β, adopts this orientation. The sheets of classes 7 and 8, like those of the 'parallel' classes 1–4, contain β-strands in register, but within each sheet, adjacent strands run in opposite directions. Antiparallel β-sheets in amyloid-like fibrils have been anticipated from previous

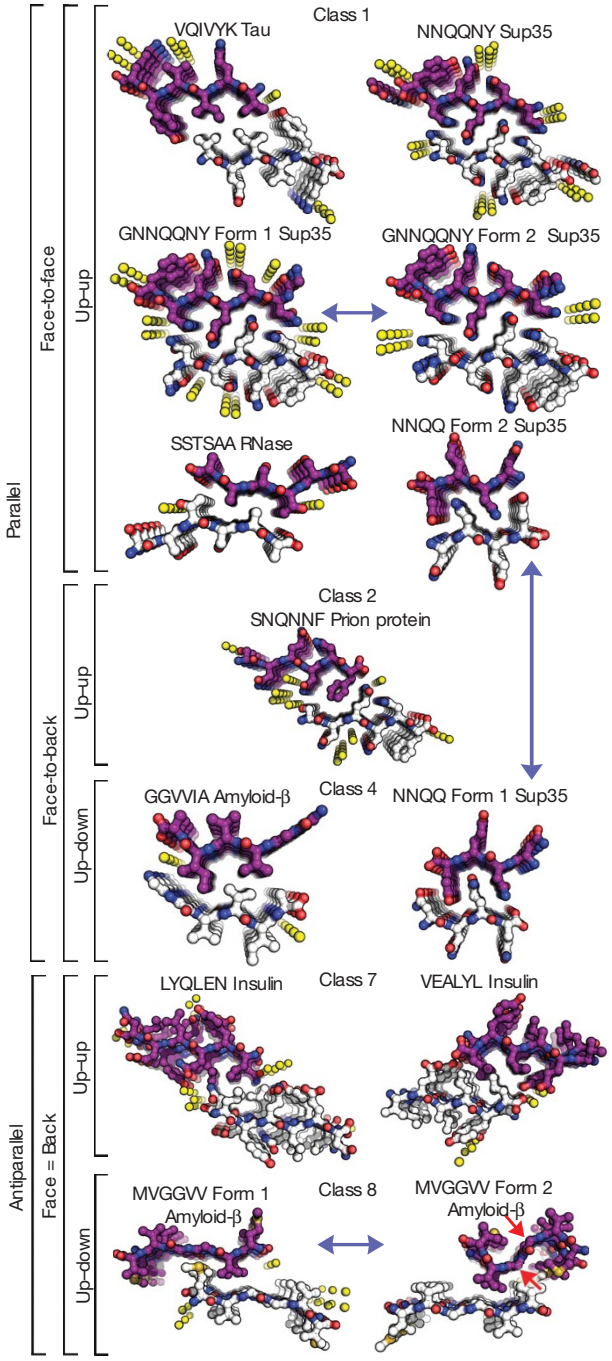

Figure 2 | Thirteen atomic-resolution structures for peptide segments of fibril-forming proteins. See text for details of nomenclature. A two-sheet motif of each structure is depicted in projection down the needle crystal axis, showing only the top members of ~10^5 stacked segments in each crystalline sheet. A dry, steric-zipper interaction is evidenced by the interdigitation of side chains between sheets. Carbon atoms are shown as purple or white, nitrogen as blue, and oxygen as red. Water molecules are shown as yellow spheres. NNQQNY also contains zinc acetate. Zippers are grouped by class (1, 2, 4, 7, 8); see text for details. Previously reported Sup35 zippers[22] belong to class 1. The three pairs of structures related by blue double-headed arrows are polymorphic pairs (forms 1 and 2; see text for details). The red arrows point to the 90° bend in the upper sheet of MVGGVV form 2.

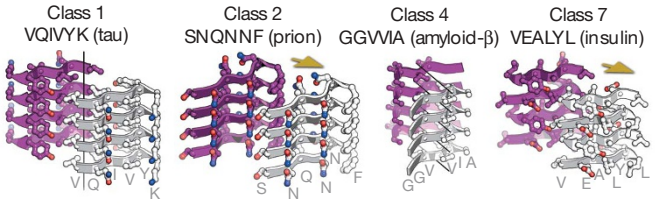

Figure 3 | 3D views of representative steric zipper structures of classes 1, 2, 4 and 7, showing the front sheet in silver and the rear sheet in purple. Oxygen atoms are red; nitrogen atoms are blue. Black lines show crystallographic 2_1 symmetry axes, and the yellow arrows show translational symmetry. The value of the shape complementarity parameter[46], S_C, for GGVVIA ($S_C = 0.92$) is the largest value we have found for any protein interface, consistent with the higher toxicity and lower solubility of amyloid-β(1−42) than (1–40).

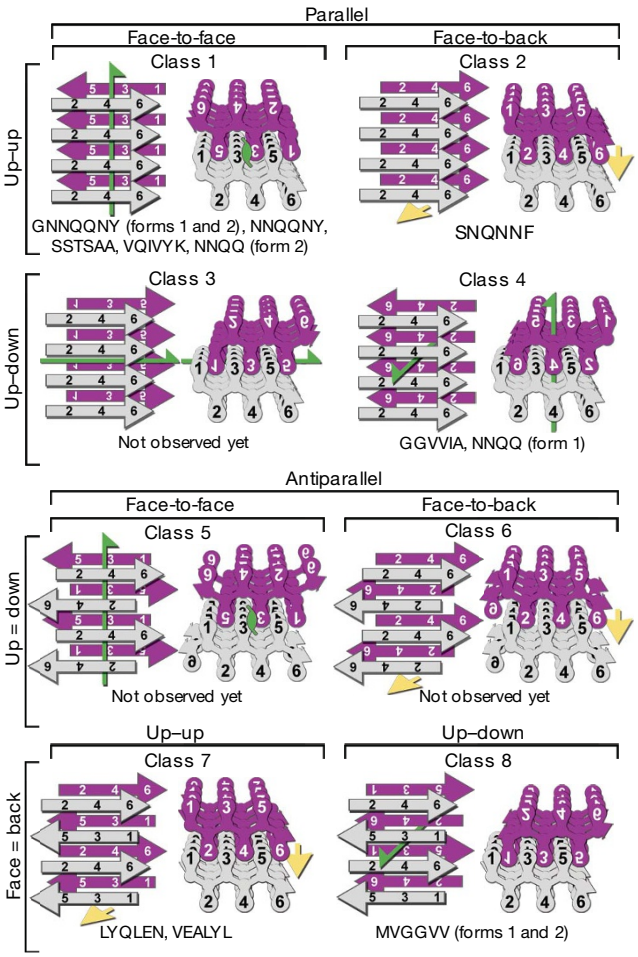

Figure 4 | The eight classes of steric zippers. Two identical sheets can be classified by: the orientation of their faces (either 'face-to-face' or 'face-to-back'), the orientation of their strands (with both sheets having the same edge of the strand 'up', or one 'up' and the other 'down'), and whether the strands within the sheets are parallel or antiparallel. Both side views (left) and top views (right) show which of the six residues of the segment point into the zipper and which point outward. Green arrows show two-fold screw axes, and yellow arrows show translational symmetry. Below each class are listed protein segments that belong to that class.

X-ray diffraction studies[33–36]. 'Face-to-back' and 'Face=back' arrangements (classes 2, 4, 6 and 8) lead naturally to adhesion of further β-sheets, favouring macroscopic tubes and sheets (for example, LYQLEN, Fig. 1a), as well as the fibrils usually seen with the pair-of-sheets motif of class 1 (Fig. 1a). To date, we have not encountered microcrystals with steric zippers of classes 3, 5 or 6.

Multiple segments and prion strains

In identifying fibril-forming segments within known fibril-forming proteins (Supplementary Table 1), we found that several proteins contain more than one fibril-forming segment. Examples are Sup35, tau, amyloid-β, β_2-microglobulin, insulin, IAPP, α-synuclein and PrP. To date, we have determined structures of different segments of both insulin and amyloid-β, finding significantly different structures for segments from the same protein. For example, GGVVIA from amyloid-β forms parallel sheets, whereas the overlapping segment MVGGVV forms antiparallel sheets. Thus fibrils formed from entire proteins could conceivably contain more than a single type of paired sheets, requiring more elaborate models (see, for example, refs 37, 38). Alternatively, protein fibrils may contain sheets built from more than a single type of protein segment. Yet another possibility is polymorphic fibrils of the same protein, each with its own steric-zipper structure. Full understanding of the organization of such fibrils will require structural studies of these more complex sheet structures.

Three of the segments shown in Fig. 2 each form two polymorphs, offering a glimpse of the possible molecular basis of the phenomena of prion strains and amyloid polymorphism[39–45]. In prion strains, a single protein sequence encodes different phenotypes, attributed recently to 'distinguishable, self-propagating structural features'[44] or different 'prion conformations'[45]. A possible molecular explanation for these effects is alternative steric zippers formed by the same sequence segment. For example, in Fig. 2, there are two polymorphic structures of NNQQ. In form 2 (class 1), the sheets are 'face-to-face', whereas they are 'face-to-back' in form 1 (class 4). We suggest that fibrils built on these two arrangements would be distinctly different in structure, and probably different in properties. Notice that the two polymorphs of GNNQQNY show essentially identical steric zippers, but the packing of the steric zippers within their crystals (Supplementary Fig. 3) differ. This suggests that crystal-packing forces do not substantially distort the basic structure of the steric zipper, although it is likely that the flatness of the sheets is influenced by packing forces.

In several of these crystal structures (as shown in Supplementary Fig. 3), sheet-to-sheet interactions involve more than just one zipper, which offers further possibilities for polymorphic structures. This is in contrast to the structures of GNNQQNY form 1, NNQQNY and VQIVYK, in which a single type of steric-zipper interaction accounts for the majority of the buried surface area between sheets (Supplementary Fig. 3). In the cases of MVGGVV form 1, LYQLEN and SSTSAA, the amount of buried surface area on a given β-sheet face is split roughly equally between two interfaces. In the example of NNQQ form 2, there are two different 'face-to-face' steric zippers. Such structures show multiple choices for tight packing of two sheets together, suggesting that sheets of the full-length protein could pack together in multiple ways to form polymorphic fibrils.

Discussion

When the 30 fibril-forming segments given in Supplementary Table 1 and the 13 microcrystal structures in Fig. 2 are considered together, they reinforce the hypothesis that microcrystal structures reveal fundamental structural features of amyloid fibrils. First, within each fibril-forming protein that we have examined, we can identify at least one segment of 4–12 residues which itself forms fibrils in isolation from the rest of the protein chain. That every fibril-forming protein contains a fibril-forming segment suggests that this segment may drive fibril formation of the protein. Second, as related above, the fibril-forming peptide segments are linked to fibrils of their parent proteins by structural, nucleation or mutational data, suggesting that the crystal structures reveal essential features of fibril structure, although there is no definitive proof that the atomic interactions are identical.

On the basis of the crystal structures reported here, as well as of earlier work by others, we summarize our observations of amyloid fibrils. (1) A 4–7-residue segment of sequence is sufficient to form a fibril in at least a dozen disease-related proteins. (2) The fundamental unit of amyloid-like fibrils is a steric zipper, formed by two tightly interdigitated β-sheets, with the possibility of more complicated geometries with multiple steric zippers. That is, the ~30 microcrystalline, fibril-forming segments of Supplementary Table 1 and the dry steric-zipper structures of Fig. 2 together suggest that amyloid diseases are similar not only on the fibril level, but also on the molecular level. (3) On the basis of the discovery of steric zippers in several disease-associated proteins, it seems likely that the process of fibril formation starts by the unmasking of zipper-forming segments in several identical protein molecules, permitting them to stack into β-sheets and the sheets to interdigitate. Recruitment of monomers into pre-formed fibrils is expected to be more rapid than nucleation, because recruitment requires only one molecule at a time to unmask its fibril-forming sequence, but formation of the steric-zipper nucleus requires several molecules to unmask their zipper-forming segments simultaneously. That is, the common feature of all these structures—the dry steric zipper—is compatible with slow fibril nucleation and faster fibril growth, the commonly observed kinetic characteristics of fibril formation[31]. (4) The finding of distinct crystalline polymorphs of the same zipper-forming segments offers a molecular-level hypothesis for amyloid polymorphism and prion strains, which awaits verification or disproof. (5) There are potentially eight classes of steric zippers, five of which have been experimentally confirmed.

METHODS

A full description of methods is given in Supplementary Information. Briefly, fibrils and microcrystals of the peptides were grown through the dissolution of lyophilized, synthetic peptide in water or buffers. Crystals were generally grown by the hanging drop method using standard crystallization screens. X-ray data were collected at ESRF beamline ID13, processed and scaled using standard software, and phased by molecular replacement with idealized β-strands. Thioflavin T fluorescence at 482 nm wavelength was used to monitor insulin fibril formation. Equal volumes of the various seeds were added to identical reactions, and each experiment was recorded for six replicates.

Received 30 November 2006; accepted 19 February 2007.
Published online 29 April 2007.

1. Westermark, P. Aspects on human amyloid forms and their fibril polypeptides. *FEBS J.* **272,** 5942–5949 (2005).
2. Westermark, P. *et al.* Amyloid: toward terminology clarification. Report from the Nomenclature Committee of the International Society of Amyloidosis. *Amyloid* **12,** 1–4 (2005).
3. Cohen, A. S. & Calkins, E. Electron microscopic observations on a fibrous component in amyloid of diverse origins. *Nature* **183,** 1202–1203 (1959).
4. Rochet, J. C., Lansbury, P. T. Jr., Amyloid fibrillogenesis: themes and variations. *Curr. Opin. Struct. Biol.* **10,** 60–68 (2000).
5. Astbury, W. T., Dickinson, S. & Bailey, K. The X-ray interpretation of denaturation and the structure of the seed globulins. *Biochem. J.* **29,** 2351–2360 (1935).
6. Geddes, A. J., Parker, K. D., Atkins, E. D. & Beighton, E. "Cross-β" conformation in proteins. *J. Mol. Biol.* **32,** 343–358 (1968).
7. Sunde, M. & Blake, C. The structure of amyloid fibrils by electron microscopy and X-ray diffraction. *Adv. Protein Chem.* **50,** 123–159 (1997).
8. Eanes, E. D. & Glenner, G. G. X-ray diffraction studies on amyloid filaments. *J. Histochem. Cytochem.* **16,** 673–677 (1968).
9. Sunde, M. *et al.* Common core structure of amyloid fibrils by synchrotron X-ray diffraction. *J. Mol. Biol.* **273,** 729–739 (1997).
10. Ritter, C. *et al.* Correlation of structural elements and infectivity of the HET-s prion. *Nature* **435,** 844–848 (2005).
11. Sikorski, P. & Atkins, E. New model for crystalline polyglutamine assemblies and their connection with amyloid fibrils. *Biomacromolecules* **6,** 425–432 (2005).
12. Petkova, A. T. *et al.* A structural model for Alzheimer's β-amyloid fibrils based on experimental constraints from solid state NMR. *Proc. Natl Acad. Sci. USA* **99,** 16742–16747 (2002).

13. Jaroniec, C. P. *et al.* High-resolution molecular structure of a peptide in an amyloid fibril determined by magic angle spinning NMR spectroscopy. *Proc. Natl Acad. Sci. USA* **101,** 711–716 (2004).
14. Krishnan, R. & Lindquist, S. L. Structural insights into a yeast prion illuminate nucleation and strain diversity. *Nature* **435,** 765–772 (2005).
15. Makin, O. S. & Serpell, L. C. Structures for amyloid fibrils. *FEBS J.* **272,** 5950–5961 (2005).
16. Lührs, T. *et al.* 3D structure of Alzheimer's amyloid-β(1–42) fibrils. *Proc. Natl Acad. Sci. USA* **102,** 17342–17347 (2005).
17. Török, M. *et al.* Structural and dynamic features of Alzheimer's Aβ peptide in amyloid fibrils studied by site-directed spin labeling. *J. Biol. Chem.* **277,** 40810–40815 (2002).
18. Paravastu, A. K., Petkova, A. T. & Tycko, R. Polymorphic fibril formation by residues 10–40 of the Alzheimer's β-amyloid peptide. *Biophys. J.* **90,** 4618–4629 (2006).
19. Williams, A. D. *et al.* Mapping Aβ amyloid fibril secondary structure using scanning proline mutagenesis. *J. Mol. Biol.* **335,** 833–842 (2004).
20. Kheterpal, I., Zhou, S., Cook, K. D. & Wetzel, R. Aβ amyloid fibrils possess a core structure highly resistant to hydrogen exchange. *Proc. Natl Acad. Sci. USA* **97,** 13597–13601 (2000).
21. Ferguson, N. *et al.* General structural motifs of amyloid protofilaments. *Proc. Natl Acad. Sci. USA* **103,** 16248–16253 (2006).
22. Nelson, R. *et al.* Structure of the cross-β spine of amyloid-like fibrils. *Nature* **435,** 773–778 (2005).
23. Balbirnie, M., Grothe, R. & Eisenberg, D. S. An amyloid-forming peptide from the yeast prion Sup35 reveals a dehydrated β-sheet structure for amyloid. *Proc. Natl Acad. Sci. USA* **98,** 2375–2380 (2001).
24. Diaz-Avalos, R. *et al.* Cross-β order and diversity in nanocrystals of an amyloid-forming peptide. *J. Mol. Biol.* **330,** 1165–1175 (2003).
25. Baxa, U. *et al.* Architecture of Ure2p prion filaments: the N-terminal domains form a central core fiber. *J. Biol. Chem.* **278,** 43717–43727 (2003).
26. Sambashivan, S., Liu, Y., Sawaya, M. R., Gingery, M. & Eisenberg, D. Amyloid-like fibrils of ribonuclease A with three-dimensional domain-swapped and native-like structure. *Nature* **437,** 266–269 (2005).
27. Thompson, M. J. *et al.* The 3D profile method for identifying fibril-forming segments of proteins. *Proc. Natl Acad. Sci. USA* **103,** 4074–4078 (2006).
28. Ivanova, M. I., Sawaya, M. R., Gingery, M., Attinger, A. & Eisenberg, D. An amyloid-forming segment of β2-microglobulin suggests a molecular model for the fibril. *Proc. Natl Acad. Sci. USA* **101,** 10584–10589 (2004).
29. Ivanova, M. I., Thompson, M. J. & Eisenberg, D. A systematic screen of β_2-microglobulin and insulin for amyloid-like segments. *Proc. Natl Acad. Sci. USA* **103,** 4079–4082 (2006).
30. Fändrich, M. & Dobson, C. M. The behaviour of polyamino acids reveals an inverse side chain effect in amyloid structure formation. *EMBO J.* **21,** 5682–5690 (2002).
31. Harper, J. D., Lansbury, P. T. Jr., Models of amyloid seeding in Alzheimer's disease and scrapie: mechanistic truths and physiological consequences of the time-dependent solubility of amyloid proteins. *Annu. Rev. Biochem.* **66,** 385–407 (1997).
32. Jarrett, J. T., Lansbury, P. T. Jr., Amyloid fibril formation requires a chemically discriminating nucleation event: studies of an amyloidogenic sequence from the bacterial protein OsmB. *Biochemistry* **31,** 12345–12352 (1992).
33. Sikorski, P., Atkins, E. D. & Serpell, L. C. Structure and texture of fibrous crystals formed by Alzheimer's Aβ(11–25) peptide fragment. *Structure (Camb.)* **11,** 915–926 (2003).
34. Makin, O. S., Atkins, E., Sikorski, P., Johansson, J. & Serpell, L. C. Molecular basis for amyloid fibril formation and stability. *Proc. Natl Acad. Sci. USA* **102,** 315–320 (2005).
35. Halverson, K., Fraser, P. E., Kirschner, D. A., Lansbury, P. T. Jr., Molecular determinants of amyloid deposition in Alzheimer's disease: conformational studies of synthetic β-protein fragments. *Biochemistry* **29,** 2639–2644 (1990).
36. Serpell, L. C. & Smith, J. M. Direct visualisation of the β-sheet structure of synthetic Alzheimer's amyloid. *J. Mol. Biol.* **299,** 225–231 (2000).
37. Kajava, A. V., Baxa, U., Wickner, R. B. & Steven, A. C. A model for Ure2p prion filaments and other amyloids: the parallel superpleated β-structure. *Proc. Natl Acad. Sci. USA* **101,** 7885–7890 (2004).
38. Kajava, A. V., Aebi, U. & Steven, A. C. The parallel superpleated β-structure as a model for amyloid fibrils of human amylin. *J. Mol. Biol.* **348,** 247–252 (2005).
39. King, C. Y. & Diaz-Avalos, R. Protein-only transmission of three yeast prion strains. *Nature* **428,** 319–323 (2004).
40. Tanaka, M., Chien, P., Naber, N., Cooke, R. & Weissman, J. S. Conformational variations in an infectious protein determine prion strain differences. *Nature* **428,** 323–328 (2004).
41. Petkova, A. T. *et al.* Self-propagating, molecular-level polymorphism in Alzheimer's β-amyloid fibrils. *Science* **307,** 262–265 (2005).
42. Chien, P. & Weissman, J. S. Conformational diversity in a yeast prion dictates its seeding specificity. *Nature* **410,** 223–227 (2001).
43. Jones, E. M. & Surewicz, W. K. Fibril conformation as the basis of species- and strain-dependent seeding specificity of mammalian prion amyloids. *Cell* **121,** 63–72 (2005).
44. Diaz-Avalos, R., King, C. Y., Wall, J., Simon, M. & Caspar, D. L. Strain-specific morphologies of yeast prion amyloid fibrils. *Proc. Natl Acad. Sci. USA* **102,** 10165–10170 (2005).
45. Tanaka, M., Collins, S. R., Toyama, B. H. & Weissman, J. S. The physical basis of how prion conformations determine strain phenotypes. *Nature* **442,** 585–589 (2006).
46. Lawrence, M. C. & Colman, P. M. Shape complementarity at protein/protein interfaces. *J. Mol. Biol.* **234,** 946–950 (1993).

Supplementary Information is linked to the online version of the paper at www.nature.com/nature.

Acknowledgements We thank D. L. D. Caspar, D. Anderson, D. Cascio, M. Gingery, M. Graf and K. Wüthrich for discussions, and the NSF, the NIH and the HHMI for support. S.A.S. was supported by an NSF IGERT training grant and M.I.A. by an NIH National Research Service Award.

Author Contributions M.R.S., S.S., R.N. and M.I.I contributed equally to this work.

Author Information The 11 new structures shown in Fig. 2, and their structure factors, have been deposited in the Protein Data Bank with accession codes as follows: GNNQQNY form 2, 2OMM; NNQQ form 1, 2ONX; NNQQ form 2, 2OLX; VEALYL, 2OMQ; LYQLEN, 2OMP; VQIVYK, 2ON9; GGVVIA, 2ONV; MVGGVV form 1, 2ONA; MVGGVV form 2, 2OKZ; SSTSAA, 2ONW; SNQNNF, 2OL9. In addition, at http://www.doe-mbi.ucla.edu/~sawaya/chime/xtalpept/ we offer, for each microcrystal structure, coordinates of the asymmetric unit, the unit cell, many unit cells, and a pair of sheets. This site also offers Chime pages that illustrate the steric zipper, polar zippers, crystal packing and water exclusion. Reprints and permissions information is available at www.nature.com/reprints. The authors declare no competing financial interests. Correspondence and requests for materials should be addressed to D.E. (david@mbi.ucla.edu).